NIH Public Access
Author Manuscript
Biofouling. Author manuscript; available in PMC 2014 July 01.

Published in final edited form as:
Biofouling. 2013 July ; 29(6): 629–640. doi:10.1080/08927014.2013.794456.

Specific degree-of-polymerization of A-type proanthocyanidin oligomers impacts *Streptococcus mutans* glucan-mediated adhesion and transcriptome responses within biofilms

Guoping Feng[a,‡], **Marlise I. Klein**[a], **Stacy Gregoire**[a], **Ajay P. Singh**[c], **Nicholi Vorsa**[c,d], and **Hyun Koo**[a,b,*]

[a]Center for Oral Biology, University of Rochester Medical Center, Rochester, NY, United States

[b]Department of Microbiology and Immunology, University of Rochester Medical Center, Rochester, NY, United States

[c]Department of Plant Biology and Plant Pathology, Rutgers University, New Brunswick, NJ, United States

[d]Philip E. Marucci Center for Blueberry and Cranberry Research and Extension, Rutgers University, Chatsworth, NJ, United States

Abstract

Cranberry A-type proanthocyanidins (PACs) have been recognized for their inhibitory activity against bacterial adhesion and biofilm-derived infections. However, the precise identification of the specific classes of degree-of-polymerization (DP) conferring PACs bioactivity remains a major challenge owing to the complex chemistry of these flavonoids. In this study, chemically characterized cranberries and a multistep separation and structure-determination technique were used to isolate A-type PAC oligomers of defined DP. The influences of PACs on 3D biofilm architecture and *Streptococcus mutans*-transcriptome responses within biofilms were investigated. Treatment regimens simulating topical exposures experienced clinically (twice-daily, 60 s each) were used over saliva-coated hydroxyapatite biofilm model. Biofilm accumulation was impaired while specific genes involved in bacterial adhesion, acid stress tolerance and glycolysis were affected by the topical treatments (*vs.* vehicle-control). Genes (*rmpC, mepA, sdcBB* and *gbpC*) associated with sucrose-dependent bacterial binding were repressed by PACs. PACs of DP 4 and particularly DP 8 to 13 were the most effective in disrupting bacterial adhesion to glucan-coated apatitic surface (>85% inhibition vs. vehicle-control), and gene expression (e.g., *rmpC*). This study identified putative molecular targets of A-type cranberry PACs in *S. mutans* while demonstrating that PAC oligomers with specific DP may be effective in disrupting assembly of cariogenic biofilms.

Keywords

Streptococcus mutans; biofilm; cranberry; proanthocyanidin; adhesion

[*]Corresponding author. Mailing address: University of Rochester Medical Center, 601 Elmwood Ave., Box 611, Rochester, NY 14642. Phone: (585) 273-4216. Fax: (585) 276-0190. Hyun_Koo@urmc.rochester.edu.
[‡]Present address: Department of Food Science, Cornell University, Ithaca, NY 14853.

NIH-PA Author Manuscript
NIH-PA Author Manuscript
NIH-PA Author Manuscript

NIH-PA Author Manuscript

NIH-PA Author Manuscript

NIH-PA Author Manuscript

Introduction

Biofilms are highly organized and structured microbial communities enmeshed in an extracellular matrix comprised of mainly polysaccharides and proteins (Flemming and Wingender 2010). Biofilms are the prevailing microbial life style in natural niches, causing many diseases in humans including those occurring in the mouth, such as dental caries (O'Toole et al. 2000; Hall-Stoodley et al. 2004). Dental caries is one of the most prevalent and costly biofilm-dependent oral diseases worldwide (Marsh 2003).

In the mouth, the assembly of cariogenic biofilms is a prime example of the consequences arising from interactions between bacteria (and their products) and dietary sugars on pellicle-coated tooth surfaces. Within the complex oral microbiome, *Streptococcus mutans* (the prime microbial culprit of dental caries) is not always the most abundant organism. However, it can rapidly orchestrate the formation of cariogenic biofilms when sucrose becomes available (Paes Leme et al. 2006; Klein et al. 2012). *S. mutans*-derived glucosyltransferases (Gtfs) are present in the tooth-pellicle and on microbial surfaces, producing exopolysaccharides (EPS) *in situ* (Schilling and Bowen 1992; Vacca-Smith and Bowen 1998; Gregoire et al. 2011). The EPS formed on surfaces provide avid bacterial binding sites (particularly for *S. mutans*) promoting local accumulation of microbes while forming a diffusion-limiting polymeric matrix that protects embedded bacteria (Stewart and Franklin, 2008; Xiao et al. 2012).

In parallel, sucrose (and other sugars) is also fermented by *S. mutans* and other acidogenic bacteria within the EPS-rich matrix, creating acidic microenvironments across the biofilm and at the surface of attachment (Xiao et al. 2012). The low pH environment facilitates EPS production while acid-tolerant and acidogenic flora prosper within biofilms, ensuring continued accumulation of EPS and acids that promote biofilm accretion and localized dissolution of the adjacent tooth enamel (Paes Leme et al. 2006). Once the biofilm is established, the resident bacteria become recalcitrant to antimicrobial therapies, making them difficult to remove while facilitating their virulence expression (Lewis 2001). Therefore, intervention of EPS-mediated bacterial binding and biofilm assembly could disrupt the pathogenesis of dental caries in a highly precise manner.

Cranberries are widely cultivated and consumed, particularly in the United States. Cranberry fruit are a rich source of various classes of flavonoids including the flavonols, the anthocyanins, and the proanthocyanidins that are polymeric flavan-3-ols, offering significant therapeutic potential (Cote et al. 2010). Cranberry juice and aqueous extracts have been recognized for their anti-adhesion and anti-biofilm activity against several bacterial pathogens including uropathogenic *Escherichia coli* and *Helicobacter pylori* (Howell et al. 1998; Burger et al. 2000; Liu et al. 2006; Koo et al. 2010b). The extracts also affected the swarming activity of *Pseudomonas aeruginosa* (O'May and Tufenkji 2011). Proanthocyanidins (PACs) appear to be the main bioactive flavonoid. PACs in cranberry are predominantly found in oligomeric forms (up to 13 monomeric units) with at least one A-type double interflavan linkage [epicatechin-(4β→8, 2β→O→7)-epicatechin] (Foo et al. 2000a). This double linkage affords conformational rigidity to PACs and appears to play a role in their bioactivity for anti-adhesion (Foo et al. 2000b; Howell et al. 2005). A-type PACs are uniquely found in high concentrations in cranberries, which appear to be more bioactive than B-type PACs, which lack the second interflavan linkage, found in other tannin-rich food (Foo et al. 2000b; Yanagida et al. 2000; Howell et al. 2005; Gregoire et al. 2007).

Previous studies have shown that PACs-containing extract is highly effective in inhibiting the EPS synthesis by surface-adsorbed Gtfs, and impaired the accumulation of *S. mutans*

NIH-PA Author Manuscript

NIH-PA Author Manuscript

NIH-PA Author Manuscript

biofilms on apatitic surfaces (Duarte et al. 2006). Recently, it was reported that topical application of cranberry PACs extract reduced the incidence of dental caries *in vivo* (Koo et al. 2010b). Interestingly, the PACs neither affected bacterial growth *in vitro* nor the number of viable populations *in vivo* (Duarte et al. 2006; Koo et al. 2010b). Although previous studies have shown anti-adhesion/anti-biofilm properties of cranberry extracts, the identity of the bioactive PACs and their molecular targets against *S. mutans* remain to be elucidated. The isolation of individual PAC oligomers from cranberries is challenging due to complex chemistry and multiple DPs with similar mass to charge ratios. Yet, it is a critical step for further elucidation of the mechanisms of action and standardization/characterization of this natural product, which are key factors for successful development of useful therapies to treat human diseases (Schmidt et al. 2007).

In this study, we used a chemically characterized cranberry cultivar which is clonally propagated and consisting of a single genotype. A step-wise chromatographic isolation method yielded highly reproducible PACs-enriched fraction and individual PACs. It was found that cranberry PACs modulates the expression of several virulence factors associated with sucrose-dependent adhesion. The bioactivity of individual PACs on *S. mutans* transcriptome and bacterial adhesion varied depending on their degree of polymerization (DP). The data provide insights about the potential therapeutic targets and the identity of cranberry PACs with high potency, which could be used to design new therapies to be evaluated *in vivo*.

Materials and Methods

Cranberry source and extraction

The fruit source for the PAC oligomers were from the cranberry cultivar ‘Stevens’, which were grown and harvested from the variety trial at the PE Marucci Center, Rutgers University, Chatsworth, NJ. Stevens is a genetically well defined (Fajardo et al. 2012) widely grown commercial cranberry cultivar with high flavonoid content (Vvedenskaya and Vorsa 2004). Cranberries were grown under standard (and monitored) nutritional and cultivation conditions. Plants in field plots of the cultivar ‘Stevens’ were fingerprinted using DNA SCAR profiling to confirm genotype and to confirm no contamination by genetic off-types (Polashock and Vorsa 2002).

Isolation and purification of cranberry A-type PACs oligomers

Early season harvest, prior to fruit anthocyanin synthesis, of the cultivar ‘Stevens’ were used for isolation A-type PACs. The cranberry PACs-containing fraction was obtained as described previously (Koo et al. 2010b). The purified fraction contained dimers, trimers, tetramers, pentamers, hexamers, heptamers, octomers, nonamers, decamers, and polymers 11, 12 and 13, and were devoid of any other flavonoid contaminants (e.g., flavonols, anthocyanins). Individual PACs were further isolated and purified using previously published method based on HPLC and diol gravity column chromatography (Singh et al. 2009). The purity of all isolated PAC DP classes was higher than 95% (w/w) as determined using LC-MS-MS and MALDI-TOF-MS. The treatment concentrations used for microarray analysis were 1.5 mg/ml for the purified PAC only-fraction, which was selected based on our previous study (Koo et al., 2010b). For comparing the bioactivity of the various PAC molecules of different DP, the treatment concentration was 100 μM for DP 2, DP 3, DP 4, DP 5–6 (combined 1:1 equimolar), DP 8–9 (combined 1:1), DP 10–11 (combined 1:1) and DP 12–13 (combined 1:1), which was the approximate amount present in the PAC extract. All compounds were dissolved in 15% ethanol in 2.5 mM potassium phosphate buffer, which was also used as a vehicle control; treatments with 15% ethanol did not affect the viability of *S. mutans* biofilm cells when compared to untreated *S. mutans* biofilms. The pH

NIH-PA Author Manuscript

NIH-PA Author Manuscript

NIH-PA Author Manuscript

of the treatment solutions was maintained at 6.5±0.2. Based on stability studies the isolated PACs were found to be stable at pH 6.5 with enhanced solubility.

Biofilm preparation and treatment

Biofilms of *S. mutans* were formed on saliva coated hydroxyapatite (sHA) surface (12.7 mm in diameter, 1 mm in thickness, Clarkson Chromatography Products Inc., South Williamsport, PA) as detailed elsewhere (Koo et al. 2010a). *S. mutans* UA159 (ATCC 7006)10), a cariogenic oral pathogen whose genome has been sequenced (Ajdic et al. 2002) was used in this study. The biofilms were grown in ultra filtered (10 kDa molecular-weight cut-off membrane; Prep/Scale, Millipore, MA) buffered tryptone-yeast extract broth (UFTYE; 2.5% tryptone and 1.5% yeast extract with the addition of 4.35 g/L of potassium phosphate and 1 g/L of magnesium sulfate, 7-hydrate , pH 7.0) with 1% sucrose at 37°C and 5% CO_2. Briefly, *S. mutans* at exponential growth phase was inoculated in UFTYE containing sHA discs placed vertically with a custom-made holder. Biofilms were allowed to form on sHA discs without interruption for the first 20 h. The biofilms were treated twice-daily at 10 a.m. (22 h-old) and 4 p.m. (28h-old), and an additional treatment next morning (at 10 a.m.; 46 h-old) with each of the test agents or vehicle-control. The biofilms were exposed to the treatments for 60 s, dip-washed in sterile saline solution (0.89% w/v NaCl) to remove excess agents, and then transferred to fresh culture medium (Koo et al. 2010b). The biofilm was analyzed at 44 h by confocal imaging to examine the effects on overall 3D architecture after receiving the initial topical treatments. The gene expression profile was determined following 4h after the last topical treatment at 46 h (Figure 1) to evaluate the impact of PACs on *S. mutans* within the accumulated biofilms post-treatment. The time-points represent the most active period of biofilm development process using our model, and were selected based on our recent studies on dynamics of *S. mutans* transcriptome during biofilm development and in response to topically applied agents (Klein et al. 2010; Falsetta et al. 2012)

Confocal laser scanning microscopy of biofilms

We assessed the overall effect of topical applications of PACs-fraction on 3D architecture, and the amount of EPS and bacteria biomass within intact biofilms using confocal fluorescence imaging (Xiao et al. 2012). EPS was labeled via incorporation of the Alexa Fluor 647 dextran conjugate (MW 10kDa; absorbance/fluorescence emission maxima of 647/668 nm), while *S. mutans* cells were stained with SYTO 9 (485/498 nm) (Molecular Probes Inc., Eugene, OR) as detailed elsewhere (Xiao et al. 2012). Imaging was performed using an Olympus FV 1000 two-photon laser scanning microscope (Olympus, Tokyo, Japan) equipped with a 10× (0.45 numerical aperture) water immersion objective lens. Each biofilm was scanned at 5 positions randomly selected at the microscope stage from 3 independent experiments, and confocal image series were generated by optical sectioning at each of these positions. The step size of z-series scanning was 2 μm. The confocal images were analyzed using software for simultaneous visualization and quantification of EPS and bacterial cells within intact biofilms (Koo et al. 2010a; Xiao et al. 2012). Amira 5.4.1 software (Visage Imaging, San Diego, CA) was used to create 3D renderings of each structural component (EPS and bacteria) for visualization of the biofilm architecture. COMSTAT was used to calculate the biomass and average thickness of the treated biofilms (Heydorn et al. 2000).

Biofilm RNA isolation and purification

RNA was extracted and purified using standard protocols optimized for biofilms (Cury and Koo 2007). The RNA integrity numbers of purified samples used for microarray and RT-qPCR were ≥9 as determined by microcapillary electrophoresis and Agilent 2100 Bioanalyzer (Agilent Technologies, Santa Clara, CA) (Schroeder et al. 2006). Purified RNA samples were stored with RNase-free water at −80 °C. The reference RNA that was used as

NIH-PA Author Manuscript

NIH-PA Author Manuscript

NIH-PA Author Manuscript

a normalization reference for microarray was isolated from planktonic *S. mutans* UA159 with the same method.

Microarray experiments. cDNA synthesis, labeling and microarray hybridization

Whole genomic profiling was conducted using *S. mutans* UA159 microarrays (version 3) provided by the J. Craig Venter Institute (JCVI). Details about the arrays are available at http://pfgrc.jcvi.org/index.php/microarray/array_description/Streptococcus_mutans/version3.html. The experimental RNAs from biofilms and reference RNA were used to generate cDNA according to the protocol provided by JCVI at http://pfgrc.jcvi.org/index.php/microarray/protocols.html. Purified experimental cDNAs were coupled with indocarbocyanine (Cy3)-dUTP, while reference cDNA was coupled with indodicarbocyanine (Cy5)-dUTP (Amersham, GE Healthcare, Little Chalfont, UK). Hybridizations were carried out at 42 °C for 17 h with a Maui Hybridization System (Biomicro Systems, Salt Lake City, UT). The slides were then washed according to JCVI protocols and scanned using a GenePix 4000B scanner (Molecular Devices, Sunnyvale, CA) at 532 nm (Cy3 channel) and 635 nm (Cy5 channel).

Microarray data analysis

After the slides were scanned, single-channel images were loaded into JCVI Spotfinder software (http://www.tm4.org/spotfinder.html) and overlaid. A spot grid was created according to JCVI specifications and then manually adjusted to fit all spots within the grid. The intensity values of each spot were measured and saved into ".mev" files. Data were normalized using LOWESS and standard deviation regularization with default settings, followed by in-slide replicate analysis using the JCVI microarray data analysis software MIDAS (http://www.tm4.org/midas.html). Spots that were flagged as having either low intensity values or low signal saturation were automatically discarded. The statistical analysis was carried out using BRB-ArrayTools (version 3.8.1; http://linus.nci.nih.gov/BRB-ArrayTools.html) with a cutoff *P* value of 0.001 for class prediction and *P* value of 0.001 and 0.01 for class comparison. A total of 4 microarray slides pairs were selected by BRB for class comparison analysis. MDV (available from LANL Oralgen http://www.oralgen.lanl.gov/) was used to assign gene names and functional classes to identified genes, as described previously (Klein et al. 2010). Genes were then sorted in Microsoft Excel to identify those with an absolute fold-change of 1.6 (up-regulation) and higher, or 0.8 (down-regulation) and lower, compared to the vehicle control. The transcriptome data were organized into the following biological themes: EPS (genes involved in biofilm matrix production), biofilm/adhesion (genes involved in biofilm formation that do not play a specific role in matrix production), glycolytic pathways (genes with known functions in sugar metabolism), stress (genes with known functions in the stress response, including oxidative stress and acid tolerance response), regulators (genes with known regulatory functions), others (with known biological function but unknown role in biofilm formation/infection), and genes encoding hypothetical proteins (genes lacking an identified function). Furthermore, we also took into account the potency of the transcriptional change by sorting genes according to their magnitude of fold-change (treatment/vehicle). cDNA microarray data have been deposited in the NCBI Gene Expression Omnibus (GEO) database (http://www.ncbi.nlm.nih.gov/geo) under GEO accession number GSE40172.

Reverse Transcription Quantitative PCR (RT-qPCR)

We performed RT-qPCR to validate and further verify the expression of specific genes selected from microarray data analysis. cDNAs were synthesized from 1 μg of purified RNA using a BioRad iScript cDNA synthesis kit (Bio-Rad Laboratories, Inc., Hercules, CA). RNA samples without reverse transcriptase were included as a negative control. The resulting cDNA and negative controls were amplified by a MyiQ qPCR detection system

NIH-PA Author Manuscript

NIH-PA Author Manuscript

NIH-PA Author Manuscript

with iQ SYBR Green supermix (Bio-Rad Laboratories, Inc., CA, USA) and specific primers (Table 1). When Taqman probes were available, cDNAs and controls were amplified using a Bio-Rad CFX96 system (Bio-Rad Laboratories). The 16S rRNA primers/TaqMan probes were run separately, and primers/TaqMan probes for other specific targets were combined and used in a multiplex setting. For reactions with only one TaqMan probe (used for target 16S rRNA) we used iQ Supermix (BioRad). For multiplex reactions (*gtfB, gtfC, gtfD* and *fruA* and, *dexA* and *ftf*) we used iQ Multiplex Powermix (BioRad). Primer and TaqMan probes sequences can be found in Table 1. Standard curves were used to determine the relative number of cDNA molecules, which were normalized to the relative number of 16S rRNA cDNA in each sample, as previously described (Yin et al. 2001). 16S rRNA served as a reference gene (Klein et al. 2010). These values were used to determine the fold of change between each treated sample and the vehicle control. The MIQE guidelines (Bustin et al. 2009) were followed for quality control of the generated data and data analysis.

Glucan-mediated bacterial adherence

The bacterial adherence assay was performed as previously described (Koo et al. 2006). The HA surfaces were coated with clarified human saliva (sHA) and glucans were formed *in situ* by surface-adsorbed GtfC in the presence of 100 mM sucrose (Koo et al., 2006) for 4h. This process ensures that sHA is completely coated with glucans (glucan-coated sHA) as determined by scanning electron and confocal fluorescence microscopy. *S. mutans* cells (1×10^9 cells) were then treated with the PAC aqueous extract or PAC molecules of DP 2 to 13, washed and incubated with glucan-coated sHA (Koo et al., 2006). After 30 min incubation, the beads were washed and the number of adherent bacteria was determined by scintillation counting (Schilling and Bowen, 1992).

Statistical analyses

Exploratory analysis was performed to assess the normality of data sets. For microarray analysis, pair-wise comparison was performed to test treatment *vs.* vehicle control. Type I error of $P<0.05$ for one-way analysis of variance was used to reject null hypothesis for biofilm structural quantitation, RT-qPCR and adhesion assays. SAS version 9.2 (SAS Institute, Cary NC) was used for all analyses.

Results and Discussion

This study isolated A-type PACs of various DP classes from a standardized single cranberry genotype, cv. Stevens, which has high flavonoids content (Vvedenskaya and Vorsa 2004). The Stevens variety has been also genetically characterized (Fajardo et al. 2012; Polashock and Vorsa 2002) and the major flavonoid classes during fruit maturation determined (Vvedenskaya and Vorsa 2004); enabling, the timing of fruit harvest to maximize the extraction and isolation of PACs. Such approaches would eliminate confounding genetic variation that could result in potential chemical and bioactivity variation commonly associated with natural products research while helping to precisely identify the bioactive molecules and the putative targets.

Topical applications of PACs affect biofilm accumulation and 3D architecture

We first examined the impact of chemically characterized and purified PACs-containing fraction on EPS-mediated biofilm assembly. We simulated clinical conditions of typical exposure of exogenously introduced therapeutic agents in the mouth by applying the extract topically twice daily for brief exposures (60 s) after initial biofilm formation (22 h-old). The typical biofilm architecture prior to treatment (22 h) is shown in Figure S1. The biomass and thickness of both EPS (red) and adherent bacteria (green) in PACs-treated biofilms were

NIH-PA Author Manuscript

NIH-PA Author Manuscript

NIH-PA Author Manuscript

significantly less than in vehicle-treated biofilms (Table 2), which resulted in defective biofilm accumulation and altered 3D architecture (Figure 2).

Confocal images revealed a marked (albeit not complete) impairment of EPS-matrix development (Figure 2), which contained approximately 3.5 times less EPS with reduced thickness (vs. vehicle-treated biofilms; Table 2). The data agree well with effective inhibition of glucan synthesis by surface-adsorbed GtfB and GtfC by cranberry PACs (Duarte et al. 2006). Such effects can greatly influence the pattern of bacterial binding and accumulation. Glucans produced on the pellicle by surface-adsorbed GtfC promotes initial bacterial adhesion while the polymers formed by GtfB bound to bacterial surface helps to further aggregate, forming cohesive microcolonies (Xiao et al. 2012). This sucrose-dependent mechanism is favorable for *S. mutans* as this bacterium expresses multiple glucan binding proteins (Sato et al. 1997; Lynch et al. 2007).

The fluorescence imaging shows that the formation and further accumulation of new microcolonies (green) were remarkably disrupted following PACs treatment (vs. vehicle-control), likely associated with reduction of EPS synthesis *in situ.* Deletion of both *gtfB* and *gtfC* in *S. mutans* completely impaired the ability of the mutant strain to assemble microcolonies even in the presence of sucrose (Xiao et al. 2012). However, it is possible that bacterial adhesion to EPS may be impaired as large areas of EPS were devoid of any attached cells or cell-clusters (Figure 1).

The development of EPS-enmeshed microcolonies is critical for the expression of biofilm virulence. These structures act as diffusion-limiting barriers facilitating the creation of highly acidic microenvironment at the surface of biofilm attachment (Xiao et al. 2012), which could promote demineralization of the adjacent tooth-enamel. The few (and sparsely distributed) microcolonies remaining in the PACs-treated biofilms appears to be larger (with higher EPS to bacteria ratio) than those in the vehicle-treated biofilms (and vs. biofilms pre-treatment at 22 h; Figure S1), suggesting that microcolony development was not completely inhibited. However, it is also apparent that there is much less EPS surrounding these microcolonies, particularly in the outer layers (Figure 2). Such biofilm architecture (with large areas devoid of microcolonies) would be less capable of maintaining acidic pH at the surface of attachment (Xiao et al. 2012). Whether the remaining microcolonies can cause enamel demineralization awaits further evaluation.

Previous studies have shown that PACs-containing extracts have no effect on growth and viability of *S. mutans* (Koo et al. 2010b) and *Candida albicans* (Feldman et al. 2012). However, it is possible that PACs could affect the expression of EPS synthesizing Gtfs or the EPS-mediated bacterial adhesion factors (critical for microcolony assembly).

PACs mostly represses gene expression by S. mutans within biofilms post-treatments

We used microarrays and multiplex RT-qPCR to characterize how topical application of PACs influences *S. mutans* transcriptome within biofilm. RT-qPCR was necessary to assess the transcriptional profiles of EPS-associated genes (*gtfBCD*, *ftf, dexA* and *fruA*), as microarrays have low confidence in detecting their mRNA levels, particularly if they are repressed (Klein et al. 2010). We detected 119 genes whose expression was differentially regulated in response to PACs. To evaluate the data generated from microarray and RT-qPCR analysis, genes were organized into categories relevant to *S. mutans* biofilm formation, fitness and virulence expression (see Materials and Methods).

There were far more repressed than induced genes (Figure 3), suggesting that upon exposure to cranberry PACs, genes associated with many cellular activities during biofilm development were more down-regulated than up-regulated. The expression levels of selected

NIH-PA Author Manuscript

NIH-PA Author Manuscript

NIH-PA Author Manuscript

genes detected by microarray were validated by RT-qPCR (Table 3). The microarray-qPCR data showed a large number of genes affected by PACs have unknown function related to biofilm formation or expression of virulence. We are currently investigating whether these genes have any significant role in *S. mutans* biofilm development. For example, *patB* (*SMU. 940*) expression was highly affected following PACs treatment. Recently, we generated a knockout mutant of *patB* from *S. mutans* UA159; initial analysis showed that gene deletion does not cause growth defect, but the strain formed less biofilms with reduced amounts of EPS (vs. parental strain) (Falsetta et al. 2012). Although further characterization is needed, it appears that *patB* may be involved with EPS synthesis during biofilm formation. It is possible that *patB* may be induced to compensate for the lack of EPS in the PACs-treated biofilms.

PACs affects expression of sucrose-dependent adhesion factors but not the expression of EPS-related enzymes

The EPS (glucans) produced from sucrose by Gtfs present on tooth-pellicle and bacterial surfaces act as binding sites (Schilling and Bowen 1992), promoting specific and avid adhesion by *S. mutans* through membrane-associated glucan-binding proteins and other co-factors (Banas and Vickerman 2003). We examined whether PACs disrupt the transcription of relevant genes associated with these sucrose-dependent processes.

The data show a major group of sucrose-dependent adhesion factors repressed by PACs treatment (Table 3). These factors include *gbpC, rmpC*, *mepA* and *sdcBB*, which play significant roles in bacterial adherence and subsequent formation of *S. mutans* biofilms in the presence of sucrose. The gene *gbpC* encodes glucan binding protein C which has been defined to be a critical contributor to *S. mutans* biofilm development and maintenance of its 3D architecture (Sato et al. 1997; Lynch et al. 2007). MepA, RmpC, SdcBB were identified as membrane-associated sucrose-dependent adhesion factors in addition to the Gbp family (Tao and Tanzer 2002). Insertional inactivation of these genes resulted in deficiency in bacterial adhesion *in vitro* and colonization of tooth surface *in vivo* in the presence of sucrose despite normal Gtf production and activity. This is the first report showing the molecular impact of cranberry PACs on the expression of biofilm-related adhesion factors by *S. mutans*.

In contrast, our study did not find significant difference in expression of genes associated with EPS synthesis (*gtfBCD*) and degradation (*dexA* and *fruA*) between the vehicle control and PACs treatments (Figure S2). Therefore, the overall reduction of EPS synthesis may be primarily due to inhibitory effects of the PACs directly on the enzymatic activity of GtfB and GtfC as evidenced by previous reports (Duarte et al. 2006; Gregoire et al. 2007; Koo et al. 2010b) but not the repression of transcription.

The extracellular effects on glucan synthesis combined with transcriptional repression of sucrose-mediated adhesion provide a fundamental interpretation of our previous data showing that cranberry crude extracts reduce bacterial adherence to glucan-coated apatitic surfaces and biofilm formation without antibacterial activity (Duarte et al. 2006; Koo et al. 2006; Gregoire et al. 2007; Koo et al. 2010b).

PACs affects expression of other relevant genes associated with biofilm virulence

We also found another group of repressed genes that are linked with glycolysis and acid stress response in *S. mutans* (Table 3). The expression of *adhE* and *citZ* was down-regulated by the PACs fraction. The genes *ahdE* and *citZ* encode alcohol-acetaldehyde dehydrogenase and citrate synthase, which are important metabolism-related enzymes in the glycolytic pathways. AdhE catalyzes the reaction of converting acetyl-CoA to ethanol and CoA

NIH-PA Author Manuscript

NIH-PA Author Manuscript

NIH-PA Author Manuscript

(Kessler et al. 1992). The *cit* operon encodes proteins for the citrate pathway and for the synthesis of the glutamate in minimal medium where organic nitrogen source is limited (Cvitkovitch et al. 1997). The gene *citZ* was also found to be a stress-responsive gene to osmolarity (Chia et al. 2001). The gene *hrcA* also appears to be repressed after exposure to PACs fraction (albeit it was not confirmed via RT-PCR). HrcA is a transcriptional regulator of *dnaK* and *groE,* which which encode important chaperones that play critical roles in helping *S. mutans* to cope with acidic stress (Jayaraman et al. 1997; Lemos et al. 2001; Lemos et al. 2007).

Conversely, *clpE* and *sodA* were induced by the PAC treatment. ClpE belongs to the Clp system which consists of proteases for degrading or chaperoning incorrectly folded proteins under acidic environment (Kajfasz et al. 2009). Gene *sodA* encodes superoxide dismutase which provides protection against oxidative stress (Nakayama 1992). The up-regulation of these genes may suggest mobilization of some of the stress response factors in order for the cells in the treated biofilms, which are less protected by EPS, to cope with the stresses. Collectively, these transcriptional changes may explain why PACs treatments reduced (albeit moderately) the acid production and acid-tolerance of *S. mutans* biofilms (Duarte et al. 2006; Gregoire et al. 2007)

Bioactivity of isolated cranberry PACs with varying degree of polymerization (DP)

The major disruptive effects caused by topical applications of cranberry PACs-fraction appears to be on the assembly of EPS-matrix and EPS-mediated processes involved in S*. mutans* adhesion and biofilm development. Several sucrose-dependent adhesion factors were repressed following topical exposure to PACs. However, cranberry PACs contained in the fraction is a mixture of molecules with variable DP. The PACs range in DP from 2 to 13 epicatechin units. Therefore, their individual bioactivity and the role of DP on *S. mutans* binding to glucan-coated surfaces and on gene expression in biofilms were assessed.

Glucan-mediated bacterial adhesion—The influence of compounds of varying DP on bacterial binding to glucan-coated apatitic surface was investigated. Specific PAC oligomers with DP>8 were potent inhibitors of *S. mutans* adhesion (as high as 85% inhibition). Generally, the bioactivity of PACs increase with higher number of epicatechin units in the molecule, but it is not linear. There is an increased effectiveness from DP 2 to 4 and DP 5 to DP 13. However, a clear distinction of bioactivity was observed for molecules of higher DP (DP>8) when compared to smaller oligomers (DP 2 to DP4) (Figure 4). The inhibitory activity from highest to lowest effect (vs. vehicle control) was DP 10–11 (85.9%, percentage of inhibition), DP 8–9 (65.7%), DP 12–13 (58.3%), DP 4 (28.7%) and DP 3 (15.7%). None of the isolated PACs caused bacterial aggregation (as observed under phase-contrast microscope) and precipitation.

The failure of inhibition by DP 5–6 is particularly intriguing, especially considering the overall trend of increased effectiveness with higher DP. Oligomers can exist in various conformations as to whether units are linked by C(4)-C(8) versus C(4)-C(6) bonds, and the location of the double A-type linkage. Additional studies shall identify the linkages of DP 5–6 oligomers relative to the DP3–4 as well DP>6 to determine potential differences in structure/conformation of these DP classes, which could be linked with bioactivity.

Gene expression—The genes *rmpC* and *hrcA* were selected based on the microarray analysis, and relevance to sucrose-dependent biofilm formation and aciduricity (Jayaraman et al. 1997; Tao and Tanzer 2002). The results from RT-qPCR analysis followed a similar trend of inhibition (vs. DP) as observed with bacterial adhesion assays. There is trend of increased effectiveness between DP 2 to 4, and from DP 5 to 13 (albeit mostly incremental)

NIH-PA Author Manuscript

NIH-PA Author Manuscript

NIH-PA Author Manuscript

(Figure 5). For the PACs with DP ranging from 2 to 4 epicatechin units, the reduction in the expression of *rmpC* and *hrcA* appeared to be correlated with increasing DP, with DP 4 being the most effective (Figure 5). The PACs with DP 5 to 10–11 displayed similar activities. There was a significant increase in repression with the DP 12–13 class. The expression profile of these two genes indicated that DP 4 and DP 12–13 was the most effective cranberry PACs in modulating the expression of selected genes of *S. mutans* biofilms. It is apparent that the specific isolated PACs are more active than the PACs-fraction in disrupting S. mutans gene expression (particularly *hrcA*). The extract contains a mixture of active and less-active PACs, which may affect the overall bioactivity (vs. individual compounds). The isolated PACs were devoid of any significant effects on the viability of *S. mutans* biofilms cells (Figure S3).

Collectively, the data show some evidence of structure-activity relationship of cranberry PAC molecules. There is a trend of increased bioactivity with higher DP (number of epicatechin units), particularly in glucan-mediated bacterial adhesion. But this relationship appears to be present in two DP ranges: DP 2 to 4 and DP 5 to 13. In each range, DP 4 and DP 12–13 (or DP 10–11 for adhesion assay) were the most effective molecules. PACs are well recognized for their interactions with proteins (Bennick 2002; Jobstl et al. 2004). Procyanidin dimers linked through a C(4)-C(8) interflavanoid bond were reported to have greater ‘tannin specific binding activity’ than dimers with C(4)-C(6) linkage (de Freitas and Mateus 2001). Besides having the A-type interflavanoid linkage cranberry trimmers were all identified to have the C (4)-C(8) linkage (Foo et al. 2000b). Larger and more complex polyphenols (DP > 8) interact more strongly and have greater protein binding activity than smaller oligomers (Baxter et al. 1997).

It is plausible that the oligomers of differing DP in this study exert their effect by more than one mechanism. The effect on adhesion could be an outcome of the effect on gene expression as well as the direct interaction of PACs with glucan-producing enzymes (Gtfs) and with *S. mutans* surface-associated glucan-binding proteins (Gbps). The DP 3–4 classes may exert most of the activity on gene expression, whereas DP > 8 involves direct protein-PAC interactions. It is possible that the lack of effect on adhesion with DP 5–6 class is that it has lesser impact on both of these mechanisms. The exact reason why these compounds have such a structure-activity relationship is unclear. It could be a result of the interplay between the degree-of-polymerization with other factors, including the molecular structure itself (e.g., the position of A-type double linkage), the location of C(4)-C(6)/C(4)-(8) linkages and the size of the molecules (which may cause strong steric hindrance). How these factors interact to each other and influence bioactivity need to be investigated in future studies.

Overall, the mechanisms of action by which topical applications of A-type PACs disrupt biofilm accumulation are quite intriguing as the expression of several sucrose-dependent bacterial adhesion factors was repressed while those associated with EPS-synthesis were unaffected. However, PACs can inhibit the activity of EPS-producing enzymes extracellularly (Duarte et al. 2006; Koo et al. 2010b). Furthermore, the expression of specific genes associated with acid stress and glycolysis was also repressed. Further analysis with purified compounds revealed that oligomers with DP 4 and DP 8 to 13 were most active in disrupting glucan-mediated bacterial adhesion and gene expression while dimers and those with DP 5–6 were generally inactive. Identification of the compounds of highest bioactivity would facilitate designing effective anti-biofilm therapies based on cranberry PACs while providing the basis for additional structure-activity studies to further elucidate the mechanisms of action of these promising non-bacteriocidal biofilm inhibitors.

NIH-PA Author Manuscript

NIH-PA Author Manuscript

NIH-PA Author Manuscript

Supplementary Material

Refer to Web version on PubMed Central for supplementary material.

Acknowledgments

This work was supported by NIH grant 5R01DE016139. The authors thank the Multiphoton Core Facility of the University of Rochester Medical Center, for their technical assistance. APS and NV are thankful to Sneha Shah and Susan Butterworth for their help in isolation of PACs.

References

Ajdic D, McShan WM, McLaughlin RE, Savic G, Chang J, Carson MB, Primeaux C, Tian R, Kenton S, Jia H, et al. Genome sequence of *Streptococcus mutans* UA159, a cariogenic dental pathogen. Proc Natl Acad Sci U S A. 2002; 99(22):14434–14439. [PubMed: 12397186]

Aoki H, Shiroza T, Hayakawa M, Sato S, Kuramitsu HK. Cloning of a *Streptococcus mutans* glucosyltransferase gene coding for insoluble glucan synthesis. Infect Immun. 1986; 53(3):587–594. [PubMed: 3017865]

Banas JA, Vickerman MM. Glucan-binding proteins of the oral streptococci. Crit Rev Oral Biol Med. 2003; 14(2):89–99. [PubMed: 12764072]

Baxter NJ, Lilley TH, Haslam E, Williamson MP. Multiple interactions between polyphenols and a salivary proline-rich protein repeat result in complexation and precipitation. Biochemistry. 1997; 36(18):5566–5577. [PubMed: 9154941]

Bennick A. Interaction of plant polyphenols with salivary proteins. Crit Rev Oral Biol Med. 2002; 13(2):184–196. [PubMed: 12097360]

Burger O, Ofek I, Tabak M, Weiss EI, Sharon N, Neeman I. A high molecular mass constituent of cranberry juice inhibits *Helicobacter pylori* adhesion to human gastric mucus. FEMS Immunol Med Microbiol. 2000; 29(4):295–301. [PubMed: 11118911]

Bustin SA, Benes V, Garson JA, Hellemans J, Huggett J, Kubista M, Mueller R, Nolan T, Pfaffl MW, Shipley GL, et al. The MIQE guidelines: Minimum information for publication of quantitative real-time PCR experiments. Clin Chem. 2009; 55(4):611–622. [PubMed: 19246619]

Chia JS, Lee YY, Huang PT, Chen JY. Identification of stress-responsive genes in *Streptococcus mutans* by differential display reverse transcription-PCR. Infect Immun. 2001; 69(4):2493–2501. [PubMed: 11254612]

Cote J, Caillet S, Doyon G, Sylvain JF, Lacroix M. Bioactive compounds in cranberries and their biological properties. Crit Rev Food Sci Nutr. 2010; 50(7):666–679. [PubMed: 20694928]

Cury JA, Koo H. Extraction and purification of total RNA from *Streptococcus mutans* biofilms. Anal Biochem. 2007; 365(2):208–214. [PubMed: 17475197]

Cvitkovitch DG, Gutierrez JA, Bleiweis AS. Role of the citrate pathway in glutamate biosynthesis by *Streptococcus mutans*. J Bacteriol. 1997; 179(3):650–655. [PubMed: 9006016]

de Freitas V, Mateus N. Structural features of procyanidin interactions with salivary proteins. J Agric Food Chem. 2001; 49(2):940–945. [PubMed: 11262053]

Duarte S, Gregoire S, Singh AP, Vorsa N, Schaich K, Bowen WH, Koo H. Inhibitory effects of cranberry polyphenols on formation and acidogenicity of *Streptococcus mutans* biofilms. FEMS Microbiol Lett. 2006; 257(1):50–56. [PubMed: 16553831]

Fajardo, D.; Morales, J.; Zhu, H.; Steffan, S.; Harbut, R.; Bassil, N.; Hummer, K.; Polashock, J.; Vorsa, N.; Zalapa, J. Discrimination of American cranberry cultivars and assessment of clonal heterogeneity using microsatellite markers. Plant Mol Biol Rep. 2012. Available from: http://link.springer.com/article/10.1007/s11105-012-0497-4/fulltext.html

Falsetta ML, Klein MI, Lemos JA, Silva BB, Agidi S, Scott-Anne KK, Koo H. Novel antibiofilm chemotherapy targets exopolysaccharide synthesis and stress tolerance in *Streptococcus mutans* to modulate virulence expression *in vivo*. Antimicrob Agents Chemother. 2012; 56(12):6201–6211. [PubMed: 22985885]

NIH-PA Author Manuscript

NIH-PA Author Manuscript

NIH-PA Author Manuscript

Feldman M, Tanabe S, Howell A, Grenier D. Cranberry proanthocyanidins inhibit the adherence properties of *Candida albicans* and cytokine secretion by oral epithelial cells. BMC Complement Altern Med. 2012; 12:6. [PubMed: 22248145]

Flemming HC, Wingender J. The biofilm matrix. Nat Rev Microbiol. 2010; 8(9):623–633. [PubMed: 20676145]

Foo LY, Lu Y, Howell AB, Vorsa N. A-type proanthocyanidin trimers from cranberry that inhibit adherence of uropathogenic P-fimbriated *Escherichia coli*. J Nat Prod. 2000a; 63(9):1225–1228. [PubMed: 11000024]

Foo LY, Lu Y, Howell AB, Vorsa N. The structure of cranberry proanthocyanidins which inhibit adherence of uropathogenic P-fimbriated *Escherichia coli in vitro*. Phytochemistry. 2000b; 54(2): 173–181. [PubMed: 10872208]

Gregoire S, Singh AP, Vorsa N, Koo H. Influence of cranberry phenolics on glucan synthesis by glucosyltransferases and *Streptococcus mutans* acidogenicity. J Appl Microbiol. 2007; 103(5): 1960–1968. [PubMed: 17953606]

Gregoire S, Xiao J, Silva BB, Gonzalez I, Agidi PS, Klein MI, Ambatipudi KS, Rosalen PL, Bauserman R, Waugh RE, et al. Role of glucosyltransferase B in interactions of *Candida albicans* with *Streptococcus mutans* and with an experimental pellicle on hydroxyapatite surfaces. Appl Environ Microbiol. 2011; 77(18):6357–6367. [PubMed: 21803906]

Hagerman AE, Butler LG. The specificity of proanthocyanidin-protein interactions. J Biol Chem. 1981; 256(9):4494–4497. [PubMed: 7217094]

Hall-Stoodley L, Costerton JW, Stoodley P. Bacterial biofilms: from the natural environment to infectious diseases. Nat Rev Microbiol. 2004; 2(2):95–108. [PubMed: 15040259]

Hamada S, Tai S, Slade HD. Binding of glucosyltransferase and glucan synthesis by *Streptococcus mutans* and other bacteria. Infect Immun. 1978; 21(1):213–220. [PubMed: 361564]

Heydorn A, Nielsen AT, Hentzer M, Sternberg C, Givskov M, Ersboll BK, Molin S. Quantification of biofilm structures by the novel computer program COMSTAT. Microbiology. 2000; 146(Pt 10 Pt 10):2395–2407. [PubMed: 11021916]

Howell AB, Vorsa N, Der Marderosian A, Foo LY. Inhibition of the adherence of P-fimbriated *Escherichia coli* to uroepithelial-cell surfaces by proanthocyanidin extracts from cranberries. N Engl J Med. 1998; 339(15):1085–1086. [PubMed: 9767006]

Howell AB, Reed JD, Krueger CG, Winterbottom R, Cunningham DG, Leahy M. A-type cranberry proanthocyanidins and uropathogenic bacterial anti-adhesion activity. Phytochemistry. 2005; 66(18):2281–2291. [PubMed: 16055161]

Jayaraman GC, Penders JE, Burne RA. Transcriptional analysis of the *Streptococcus mutans hrcA, grpE* and *dnaK* genes and regulation of expression in response to heat shock and environmental acidification. Mol Microbiol. 1997; 25(2):329–341. [PubMed: 9282745]

Jobstl E, O'Connell J, Fairclough JP, Williamson MP. Molecular model for astringency produced by polyphenol/protein interactions. Biomacromolecules. 2004; 5(3):942–949. [PubMed: 15132685]

Kajfasz JK, Martinez AR, Rivera-Ramos I, Abranches J, Koo H, Quivey RG Jr, Lemos JA. Role of clp proteins in expression of virulence properties of *Streptococcus mutans*. J Bacteriol. 2009; 191(7): 2060–2068. [PubMed: 19181818]

Kessler D, Herth W, Knappe J. Ultrastructure and pyruvate formate-lyase radical quenching property of the multienzymic AdhE protein of *Escherichia coli*. J Biol Chem. 1992; 267(25):18073–18079. [PubMed: 1325457]

Klein MI, Xiao J, Lu B, Delahunty CM, Yates JR 3rd, Koo H. *Streptococcus mutans* protein synthesis during mixed-species biofilm development by high-throughput quantitative proteomics. PLoS One. 2012; 7(9):e45795. [PubMed: 23049864]

Klein MI, DeBaz L, Agidi S, Lee H, Xie G, Lin AH, Hamaker BR, Lemos JA, Koo H. Dynamics of *Streptococcus mutans* transcriptome in response to starch and sucrose during biofilm development. PLoS One. 2010; 5(10):e13478. [PubMed: 20976057]

Koo H, Xiao J, Klein MI, Jeon JG. Exopolysaccharides produced by *Streptococcus mutans* glucosyltransferases modulate the establishment of microcolonies within multispecies biofilms. J Bacteriol. 2010a; 192(12):3024–3032. [PubMed: 20233920]

NIH-PA Author Manuscript

NIH-PA Author Manuscript

NIH-PA Author Manuscript

Koo H, Nino de Guzman P, Schobel BD, Vacca Smith AV, Bowen WH. Influence of cranberry juice on glucan-mediated processes involved in *Streptococcus mutans* biofilm development. Caries Res. 2006; 40(1):20–27. [PubMed: 16352876]

Koo H, Duarte S, Murata RM, Scott-Anne K, Gregoire S, Watson GE, Singh AP, Vorsa N. Influence of cranberry proanthocyanidins on formation of biofilms by *Streptococcus mutans* on saliva-coated apatitic surface and on dental caries development *in vivo*. Caries Res. 2010b; 44(2):116–126. [PubMed: 20234135]

Lemos JA, Luzardo Y, Burne RA. Physiologic effects of forced down-regulation of *dnaK* and *groEL* expression in *Streptococcus mutans*. J Bacteriol. 2007; 189(5):1582–1588. [PubMed: 17172345]

Lemos JA, Chen YY, Burne RA. Genetic and physiologic analysis of the *groE* operon and role of the HrcA repressor in stress gene regulation and acid tolerance in *Streptococcus mutans*. J Bacteriol. 2001; 183(20):6074–6084. [PubMed: 11567008]

Lewis K. Riddle of biofilm resistance. Antimicrob Agents Chemother. 2001; 45(4):999–1007. [PubMed: 11257008]

Liu Y, Black MA, Caron L, Camesano TA. Role of cranberry juice on molecular-scale surface characteristics and adhesion behavior of *Escherichia coli*. Biotechnol Bioeng. 2006; 93(2):297–305. [PubMed: 16142789]

Lynch DJ, Fountain TL, Mazurkiewicz JE, Banas JA. Glucan-binding proteins are essential for shaping *Streptococcus mutans* biofilm architecture. FEMS Microbiol Lett. 2007; 268(2):158–165. [PubMed: 17214736]

Marsh PD. Are dental diseases examples of ecological catastrophes? Microbiology. 2003; 149(Pt 2): 279–294. [PubMed: 12624191]

Nakayama K. Nucleotide sequence of *Streptococcus mutans* superoxide dismutase gene and isolation of insertion mutants. J Bacteriol. 1992; 174(15):4928–4934. [PubMed: 1321118]

O'May C, Tufenkji N. The swarming motility of *Pseudomonas aeruginosa* is blocked by cranberry proanthocyanidins and other tannin-containing materials. Appl Environ Microbiol. 2011; 77(9): 3061–3067. [PubMed: 21378043]

O'Toole G, Kaplan HB, Kolter R. Biofilm formation as microbial development. Annu Rev Microbiol. 2000; 54:49–79. [PubMed: 11018124]

Paes Leme AF, Koo H, Bellato CM, Bedi G, Cury JA. The role of sucrose in cariogenic dental biofilm formation--new insight. J Dent Res. 2006; 85(10):878–887. [PubMed: 16998125]

Polashock J, Vorsa N. Development of SCAR markers for DNA fingerprinting and germplasm analysis of American cranberry. J Am Soc Hort Sci. 2002; 127(4):677–684.

Sato Y, Yamamoto Y, Kizaki H. Cloning and sequence analysis of the *gbpC* gene encoding a novel glucan-binding protein of *Streptococcus mutans*. Infect Immun. 1997; 65(2):668–675. [PubMed: 9009329]

Schilling KM, Bowen WH. Glucans synthesized *in situ* in experimental salivary pellicle function as specific binding sites for *Streptococcus mutans*. Infect Immun. 1992; 60(1):284–295. [PubMed: 1530843]

Schmidt BM, Ribnicky DM, Lipsky PE, Raskin I. Revisiting the ancient concept of botanical therapeutics. Nat Chem Biol. 2007; 3(7):360–366. [PubMed: 17576417]

Schroeder A, Mueller O, Stocker S, Salowsky R, Leiber M, Gassmann M, Lightfoot S, Menzel W, Granzow M, Ragg T. The RIN: An RNA integrity number for assigning integrity values to RNA measurements. BMC Mol Biol. 2006; 7:3. [PubMed: 16448564]

Singh AP, Singh RK, Kim KK, Satyan KS, Nussbaum R, Torres M, Brard L, Vorsa N. Cranberry proanthocyanidins are cytotoxic to human cancer cells and sensitize platinum-resistant ovarian cancer cells to paraplatin. Phytother Res. 2009; 23(8):1066–1074. [PubMed: 19172579]

Stewart PS, Franklin MJ. Physiological heterogeneity in biofilms. Nat Rev Microbiol. 2008; 6(3):199–210. [PubMed: 18264116]

Tao L, Tanzer JM. Novel sucrose-dependent adhesion co-factors in *Streptococcus mutans*. J Dent Res. 2002; 81(7):505–510. [PubMed: 12161466]

Vacca-Smith AM, Bowen WH. Binding properties of streptococcal glucosyltransferases for hydroxyapatite, saliva-coated hydroxyapatite, and bacterial surfaces. Arch Oral Biol. 1998; 43(2): 103–110. [PubMed: 9602288]

NIH-PA Author Manuscript

NIH-PA Author Manuscript

NIH-PA Author Manuscript

Vvedenskaya I, Vorsa N. Flavonoid composition over fruit development and maturation in American cranberry, *Vaccinium macrocarpon* ait. Plant Science. 2004; 167(5):1043–1054.

Xiao J, Klein MI, Falsetta ML, Lu B, Delahunty CM, Yates JR 3rd, Heydorn A, Koo H. The exopolysaccharide matrix modulates the interaction between 3D architecture and virulence of a mixed-species oral biofilm. PLoS Pathog. 2012; 8(4):e1002623. [PubMed: 22496649]

Yanagida A, Kanda T, Tanabe M, Matsudaira F, Oliveira Cordeiro JG. Inhibitory effects of apple polyphenols and related compounds on cariogenic factors of mutans streptococci. J Agric Food Chem. 2000; 48(11):5666–5671. [PubMed: 11087536]

Yin JL, Shackel NA, Zekry A, McGuinness PH, Richards C, Putten KV, McCaughan GW, Eris JM, Bishop GA. Real-time reverse transcriptase-polymerase chain reaction (RT-PCR) for measurement of cytokine and growth factor mRNA expression with fluorogenic probes or SYBR green. Immunol Cell Biol. 2001; 79(3):213–221. [PubMed: 11380673]

NIH-PA Author Manuscript

NIH-PA Author Manuscript

NIH-PA Author Manuscript

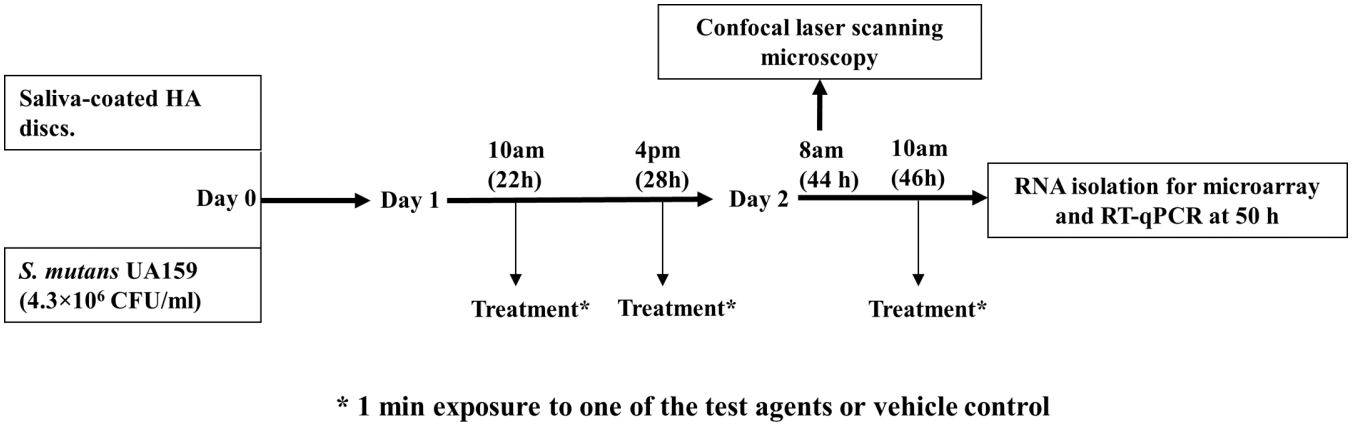

Figure 1. Experimental design for treatment and analysis of *S. mutans* biofilms

NIH-PA Author Manuscript

NIH-PA Author Manuscript

NIH-PA Author Manuscript

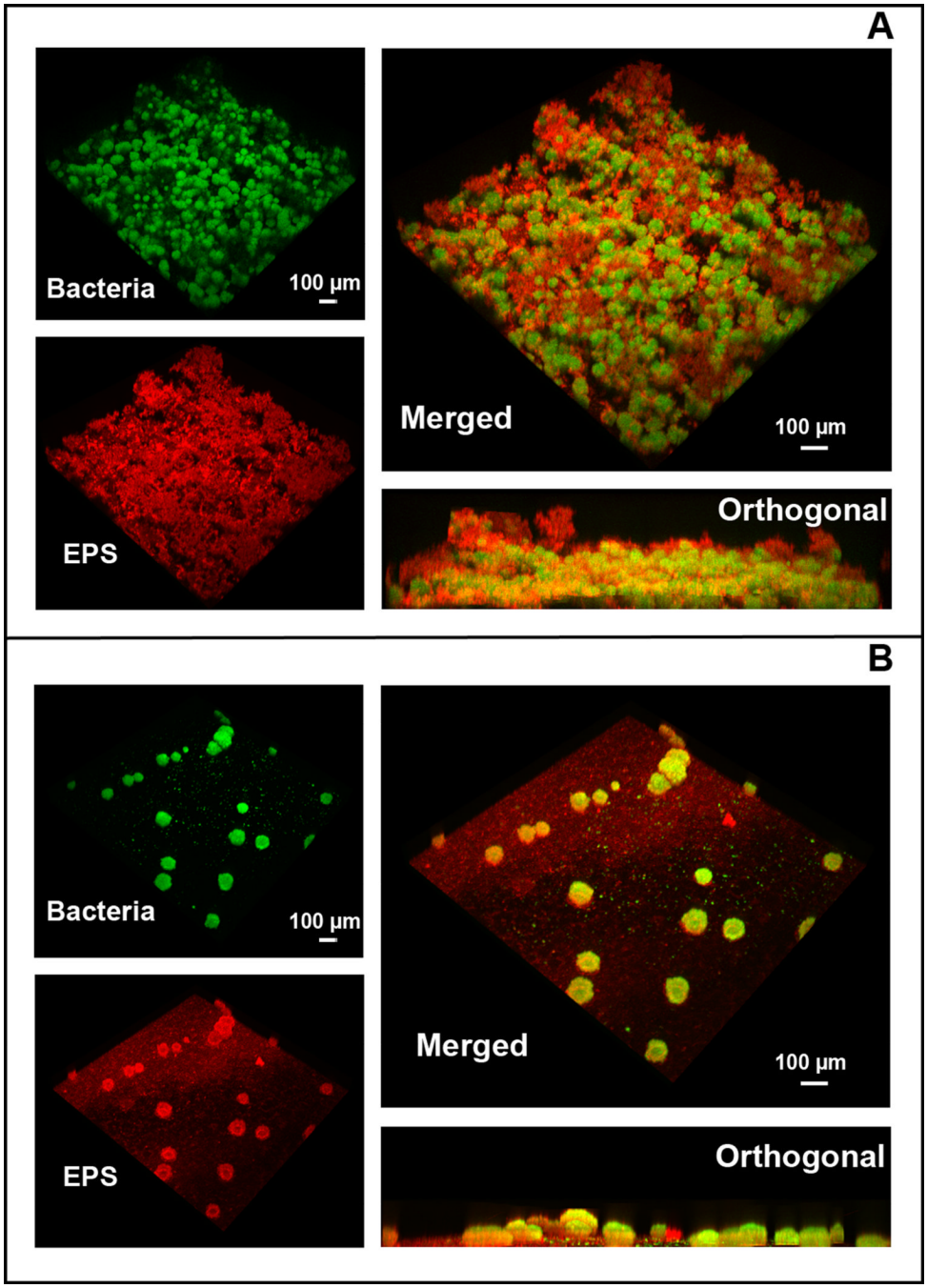

Figure 2. Representative 3D rendering images of *S. mutans* biofilms following topical treatments with vehicle-control (A) and with cranberry PACs (B)

Biofilms were treated topically with vehicle-control and PACs-containing fraction. The EPS channel is in red; bacterial cells are in green.

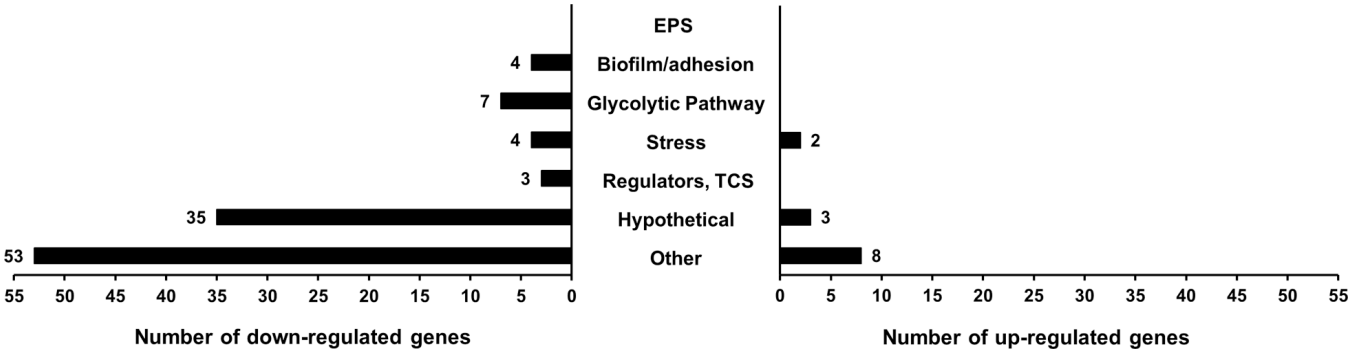

Figure 3. Functional categories affected by PACs treatment

Number of repressed (left panel) and induced (right panel) *S. mutans* genes in biofilms exposed to PACs-containing fraction (n=4). Genes are grouped into specific functional categories (biological themes) as listed in the center of the graph. Genes whose fold of change in expression was ≤0.8 or ≥1.5 ($P<0.05$) were included.

NIH-PA Author Manuscript NIH-PA Author Manuscript NIH-PA Author Manuscript

NIH-PA Author Manuscript

NIH-PA Author Manuscript

NIH-PA Author Manuscript

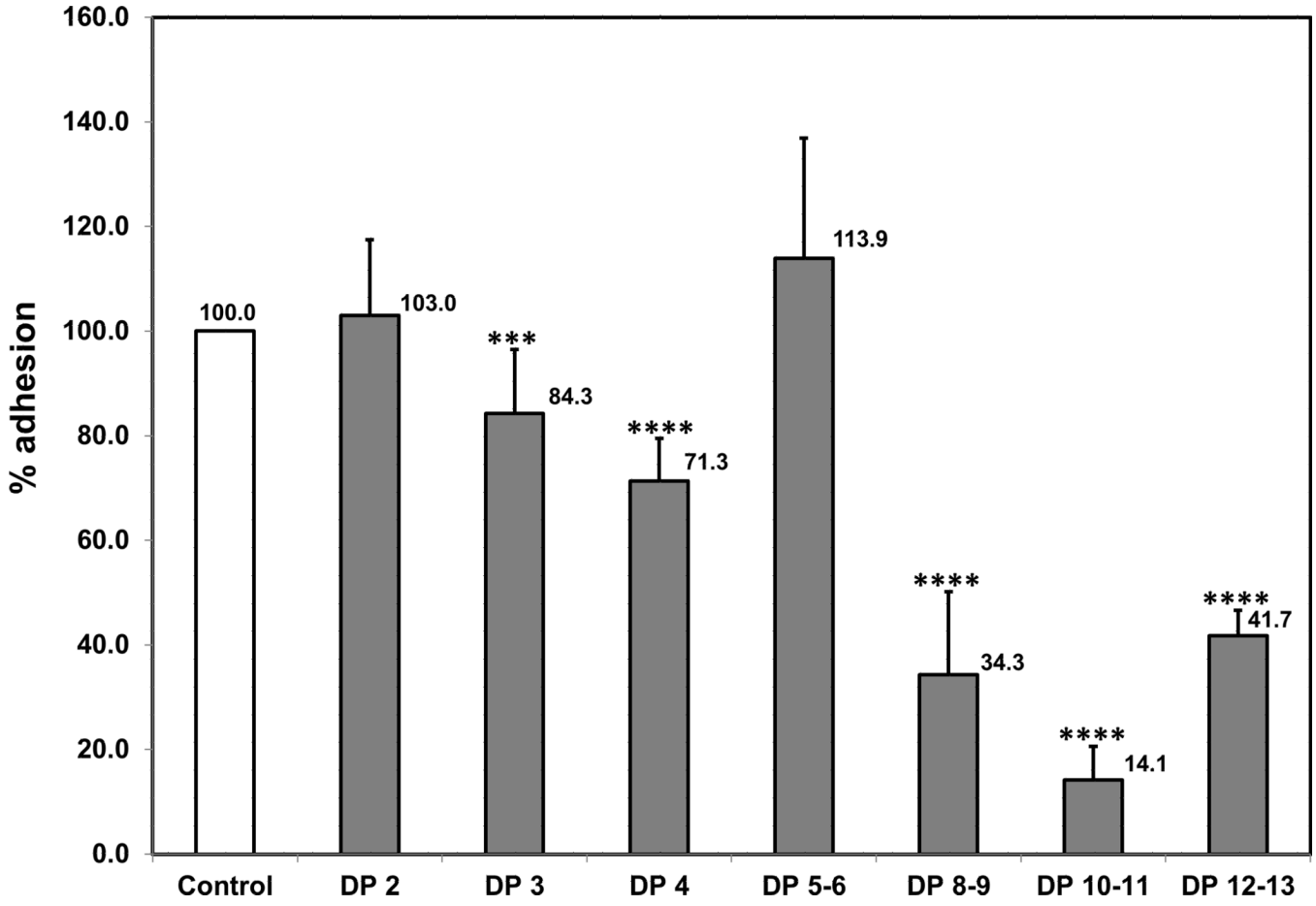

Figure 4. Adhesion of *S. mutans* cells treated with isolated PAC molecules of degree-of-polymerization (DP) 2 to 13 to glucan-coated apatitic surface

Percentage of bacterial binding was calculated considering the vehicle-control treated cell as 100% adhesion. Values with three and four asterisk are significantly different from the control at a level of $P<0.001$ and $P<0.0001$ (n=3). All the values among different DPs are significantly different from each other ($P<0.05$), except between DP 8–9 and DP 12–13 ($P>0.05$).

NIH-PA Author Manuscript
NIH-PA Author Manuscript
NIH-PA Author Manuscript

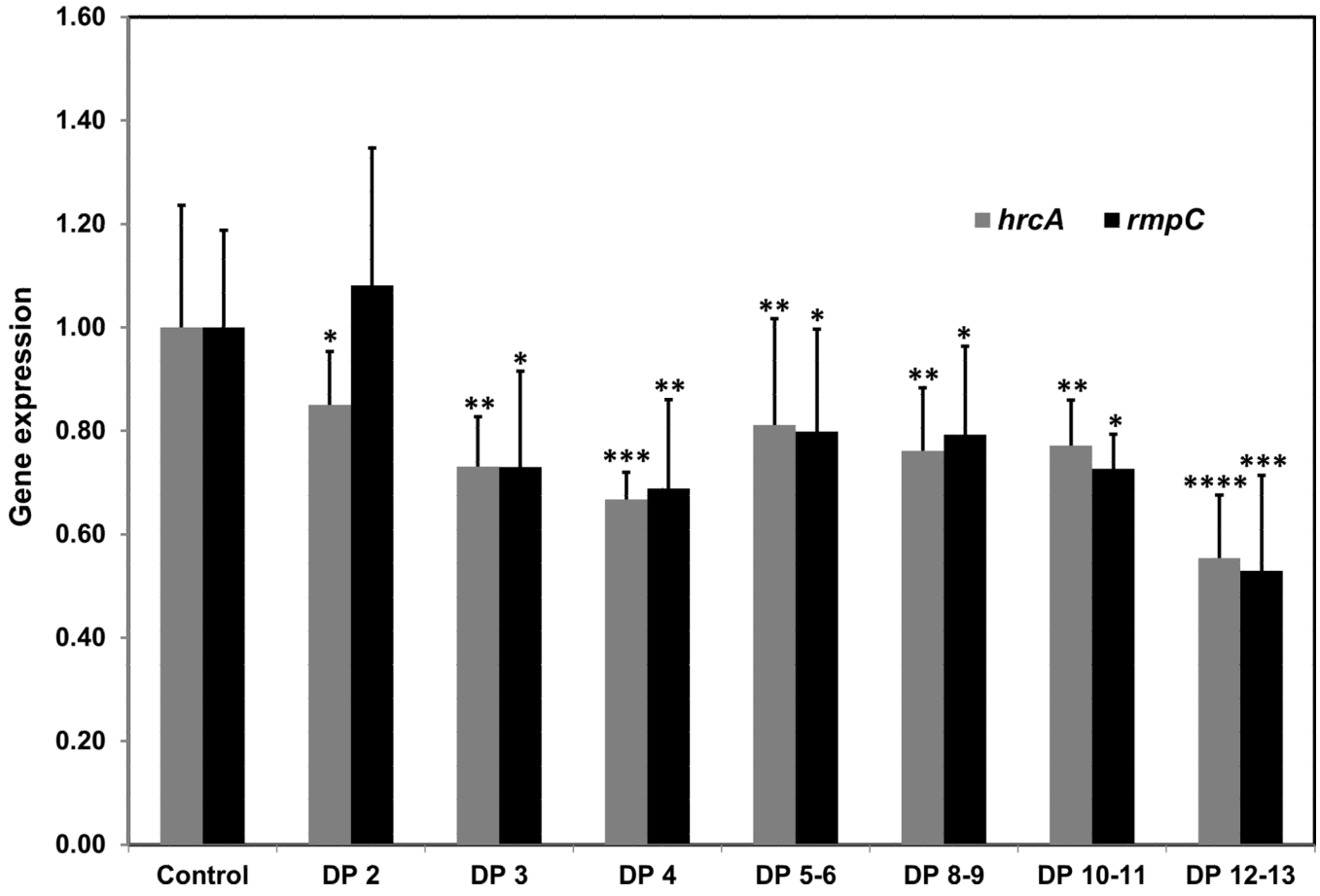

Figure 5. Gene expression of *S. mutans rmpC* and *hrcA* in biofilms topically treated with isolated PAC molecules of DP 2–13

Values marked with one, two, three and four asterisk are significantly different from the control at a level of $P<0.05$, $P<0.01$, $P<0.001$ and $P<0.0001$. For *rmpC*, value for DP 2 is significantly different from all others at a level of $P<0.05$. Values for DP 3, DP 4, DP 5–6, DP 8–9 and DP 10–11 are significantly different from DP 2 and DP 12–13 ($P<0.05$) but not from each other ($P>0.05$). Value for DP 12–13 is significantly different from all others at a level of $P<0.05$. For *hrcA,* value for DP 2 is significantly different from DP 3, DP 4 and DP 12–13 ($P<0.05$). Value for DP 3 is significantly different from DP2 and DP 12–13($P<0.05$). Value for DP 4 is significantly different from DP 2, DP 5–6, DP 8–9, DP 10–11 and DP 12–13 ($P<0.05$). Values for DP 5–6, DP 8–9 and DP 10–11 are significantly different from DP 2, DP 4 and DP 12–13 ($P<0.05$) but not from DP 3 and from each other ($P>0.05$).

NIH-PA Author Manuscript
NIH-PA Author Manuscript
NIH-PA Author Manuscript

Table 1

Primers and TaqMan probes used for RT-qPCR*

GenBank ID	Gene	Primer sequence (forward and reverse)	TaqMan probe sequence and dual-labeled probes (reporters and quenchers)	Reference
	16S rRNA	ACCAGAAAGGGACGGCTAAC TAGCCTTTTACTCCAGACTTTCCTG	CTAACGCAATAAGCACTCCGCCTGG 5' FAM / 3' BHQ-1	
SMU.1004	*gtfB*	AAACAACCGAAGCTGATAC CAATTTCTTTTACATTGGGAAG	ATTGGCTGCATTGCTATCATCA 5' HEX / 3' BHQ-1	
SMU.1005	*gtfC*	CTCTGACTGCTACTGATACAAG CCGAAGTTGTTGTTGGTTTAAC	AGCAACATCTCAACCAACCGCC 5' Cal Fluor Red 610 / 3' BHQ-2	
SMU.910	*gtfD*	AGCACAAACTTCTGAAGAGC CAGCTTTTGCCTGTGTTAAAG	CCTGTGCTTCTTCTGCTTGCTT 5' Quasar 670 / 3' BHQ-2	Xiao et al., 2012
SMU.2042c	*dexA*	TATTTTAGAGCAGGGCAATCG AACCTCCAATAGCAGCATAAC	ACGCCAGTCATCCTCAACCGCA 5' Quasar 705 / 3' BHQ-2	
SMU.78	*fruA*	AACAACTGCTGCTGATACTG CTGCGGTTTCTTGAGATGAC	TCTGGCTGCTGTCTTCTGTTCT 5' FAM / 3' BHQ-1	
SMU.2028c	*ftf*	CTGACATAACTACGCCAAAG TGCTTAAATTAATACCAGCTTC	CGCAATCTTACGAGCCTGTTCTGTT 5' HEX / 3' BHQ-1	
SMU.80	*hrcA*	AATTAGGACTCTTAGAGAAGGC AACATCCTGTTCGTCCAA	NA	
SMU.270	*rmpC*	TTGGCTTCTTCTTCAATA TAACCATCAAGGTAACTG	NA	
SMU.148	*adhE*	GCATCATTGGTGAAGATA GTTAGTTGTTGGTACGAT	NA	
SMU.2109	*mepA*	CTAGTGAGTGGACATTAG CTAATAGGTGAGGCTTAC	NA	This study
SMU.671	*citZ*	CAACGGTAAGTCTATTAGG TAATGGTCGGTATCTTGG	NA	
SMU.1396	*gbpC*	CTAAGTATGGCGATCATG ATATTGGTTGTCCTTAGC	NA	
SMU.1933c	*sdcBB*	TCCTTGGATAGAATAGATAC AAGGCTGATAAGTATACC	NA	
SMU.629	*sodA*	ATGACGCACTTGAACCATAT CTGACGAATATCCGCTGG	NA	
SMU.562	*clpE*	GCGACTATTCATCTATATGC GTCCATTTTCAGGATCTG	NA	Kajfasz et al., 2009
SMU.940	*patB*	CTTGTCTTTCATCGGTGTTCATAC GGTCGCTCGTTTGATTGTTATTAC	NA	Falsetta et al., 2012

*NA: not applicable.

All oligonucleotides were designed using the program Beacon designer (Premier Biosoft, Palo Alto, CA), synthesized and supplied by Integrated DNA Technologies (Coralville, IA).

NIH-PA Author Manuscript

NIH-PA Author Manuscript

NIH-PA Author Manuscript

Table 2

Biomass and average thickness values of bacterial cells and EPS in PACs-treated biofilms.

Treatment	biomass (μm^3)		average thickness (μm)	
	Bacteria	EPS	Bacteria	EPS
Vehicle-control	28.93±3.61[a]	68.18±7.92[a]	98.93±13.3[a]	101.2±10.53[a]
PACs	4.31±2.68[b]	19.88±7.23[b]	5.89±3.98[b]	20.82±8.51[b]

Biofilms were treated topically with vehicle-control and PACs-containing fraction. Values labeled with a different letter in each column are statistically different ($P<0.0001$, n=3).

NIH-PA Author Manuscript

NIH-PA Author Manuscript

NIH-PA Author Manuscript

Table 3

Selected genes detected in PACs-treated biofilms as differentially expressed (vs. vehicle-control) by microarray analysis.

GenBank ID	Gene	Functional category	Microarray	RT-qPCR
SMU.1396	*gbpC*	Biofilm/adhesion	0.81	0.83*
SMU.270	*rmpC*	Biofilm/adhesion	0.68	0.64*
SMU.2109	*mepA*	Biofilm/adhesion	0.72	0.70*
SMU.1933c	*sdcBB*	Biofilm/adhesion	0.74	0.69*
SMU.148	*adhE*	Glycolytic pathway	0.7	0.72*
SMU.671	*citZ*	Glycolytic pathway	0.67	0.75*
SMU.80	*hrcA*	Stress (acid)	0.76	0.89
SMU.629	*sodA*	Stress (oxidative)	1.6	1.56*
SMU.562	*clpE*	Stress (acid)	1.75	1.56*
SMU.940	*patB*	Other	1.7	2.78*

These genes were selected for RT-qPCR validation. Biofilms were treated topically with vehicle-control and PACs-containing fraction.

Values marked with an asterisk (*) are significantly different from biofilms treated with vehicle control ($P<0.05$, n=3).